Structural modification of the skin barrier by OH radicals : a reactive molecular dynamics study for plasma medicine

Reference:

Van der Paal J., Verlackt Christof, Yusupov Maksudbek, Neyts Erik, Bogaerts Annemie.- Structural modification of the skin barrier by OH radicals : a reactive molecular dynamics study for plasma medicine

Journal of physics: D: applied physics - ISSN 0022-3727 - 48:15(2015), 155202

DOI: http://dx.doi.org/doi:10.1088/0022-3727/48/15/155202

Structural modification of the skin barrier by OH radicals: A reactive molecular dynamics study for plasma medicine

J. Van der Paal, C. C. Verlackt, M. Yusupov, E. C. Neyts and A. Bogaerts

Research Group PLASMANT, Department of Chemistry, University of Antwerp, Universiteitsplein 1, B-2610 Antwerp, Belgium

E-mail: annemie.bogaerts@uantwerpen.be

Abstract. While plasma treatment of skin diseases and wound healing has been proven highly effective, the underlying mechanisms, and more in general the effect of plasma radicals on skin tissue, are not yet completely understood. In this paper, we perform ReaxFF-based reactive molecular dynamics simulations to investigate the interaction of plasma generated OH radicals with a model system composed of free fatty acids, ceramides, and cholesterol molecules. This model system is an approximation of the upper layer of the skin (stratum corneum). All interaction mechanisms observed in our simulations are initiated by H-abstraction from one of the ceramides. This reaction, in turn, often starts a cascade of other reactions, which eventually lead to the formation of aldehydes, the dissociation of ceramides or the elimination of formaldehyde, and thus eventually to the degradation of the skin barrier function.

PACS codes: 52.65.Yy, 87.10.Tf, 87.15.ap, 52.40.-w

1. Introduction

Biomedical applications of cold atmospheric plasmas (CAPs) are attracting a great deal of interest in the scientific community and are becoming one of the main topical areas of plasma research [1-6]. Nowadays, many experimental works are devoted to the treatment of biomedically relevant surfaces by CAPs. This includes sterilization or disinfection of non-living surfaces (e.g., microbial deactivation of surgical and medical tools, heat-sensitive and packaging materials, food and food product lines, as well as seeds [7-15]) and treatment of living surfaces (e.g., treatment of skin diseases, cancer treatment, blood coagulation, as well as dermatological wound healing [6, 16-21]).

CAPs produce a large variety of biomedically active agents, such as reactive oxygen species (ROS) (e.g., O, OH, H_2O_2, O_3) and reactive nitrogen species (RNS) (e.g., NO, NO_2, HNO_2). These species are thought to be the most important for biomedical applications [22]. For instance, some of the experimental studies revealed that O and OH play a dominant role in the inactivation of bacteria, whereas other plasma-generated components (e.g., UV photons, charged particles, electric fields, and heat) have a minor contribution [23-26]. CAP sources are also able to kill bacteria that cause infections in skin wounds and ulceration without having a negative effect on human tissue [27-29]. Note that the treatment of such infections with conventional antibiotics is often problematic. Thus, CAPs can be effectively used in dermatology (for skin disinfection/antisepsis), while having no damage to the sensitive surface of biomaterials. This is more likely due to their nontoxic character (i.e., they can be sustained in nontoxic gases, such as argon, hydrogen, or oxygen, which is relatively safe to e.g., medical staff, as well as to the environment) and their non-thermal nature, which is ideal for heat-sensitive materials, as the gas temperature of CAPs is below the destruction threshold.

Despite the increasing interest in CAPs for various biomedical applications, accurate control of the processes occurring in the plasma and more importantly at the surface of living cells (i.e., in the contact region of the plasma with the bio-organisms) still remains a big challenge, although some fundamental investigations were already carried out by experiments (see e.g., [30-33]).

Computer simulations, on the other hand, can provide fundamental information about processes occurring in the plasma and at the surface of living cells. However, until now only few modeling efforts have been made, especially with respect to the interaction of plasma with living organisms. A recent review provides an overview of the current state-of-the-art and possible future directions [34].

Recently, we have performed a number of reactive molecular dynamics (MD) simulations to study the interaction mechanisms of ROS with several types of relevant biomolecules at the atomic level

[35-40]. Specifically, we have investigated the interaction of ROS with peptidoglycan (an important component of the cell wall of gram-positive bacteria) [36, 37] and with lipid A (a toxic part of the outer cell wall of gram-negative bacteria) [38] as well as with a liquid water layer as a simple model system for the biofilm covering the bacteria [39]. Moreover, we have also studied the interaction of O and OH radicals with α-linolenic acid, which is a model system for the free fatty acids present in the upper skin layer [40].

In the present study, we further extend the latter work, using a more realistic model system for the upper skin layer (stratum corneum; SC), based on various experimental results [41-43]. This model system is composed of free fatty acids, ceramides, and cholesterol molecules. Although this still remains an approximation of the real system, where the stratum corneum is surrounded by a water layer and other species (e.g. RNS, O, O_2 and H_2O) are able to react with the upper skin layer, the complexity of this model has drastically improved compared to our previous study [40].

This study is of great importance to better understand the fundamental phenomena occurring in the upper skin layer upon impact of plasma generated OH radicals. For instance, it is of great interest to investigate whether plasma species can affect the skin barrier function and contribute to pore formation in the skin layer, due to the dissociation of for instance the ceramides, or whether they give rise to the formation of specific molecules, that can be either harmful or beneficial for the human body. The model system under study and the simulation setup will be explained in section 2. The calculation results will be presented in section 3, while section 4 discusses the possible implications of this study. Finally, the conclusions will be given in section 5.

2. Simulation setup

In MD simulations, the time evolution of all the atoms in the system is calculated by integrating the equations of motion. The forces acting on the atoms are obtained as the negative derivative of the interatomic interaction potential, also called "force field", between these atoms. As we are interested in the breaking and formation of bonds to investigate the damage of structures, we need to make use of a reactive force field. In this work, we use the ReaxFF potential – a classical force field, which was originally developed for hydrocarbons [44], but soon expanded to a variety of other elements. It is currently one of the most widely parameterized reactive force fields available. It accurately simulates bond breaking/formation processes, commonly approaching quantum mechanical (QM) accuracy. Thus, it serves as a link between QM and empirical (non-reactive) force fields [45]. ReaxFF is capable of describing both covalent and ionic bonds, as well as the entire range of intermediate interactions. A more detailed description of the energy terms used in ReaxFF and the parameters used in this study can be found in [46] and [47], respectively.

In this work, we study the interaction of OH radicals with a mixture of ceramides, cholesterol and free fatty acids, using reactive MD simulations. Note that the system under investigation is placed in a vacuum, *i.e.* without a surrounding water layer, making this model system an approximation of the real stratum corneum. In this real system other radicals or molecules that are created by the plasma or that are abundant in ambient air (e.g., O, O_2, H_2O or RNS) can also react with the stratum corneum. These species were, however, not investigated for the following reasons. Firstly, oxygen radicals were not investigated as preliminary results showed that they reacted according to the same reaction mechanism as OH radicals. Indeed, oxygen radicals would in the real system react with surrounding water molecules leading to the formation of new OH radicals [39]. Secondly, water and O_2 don't cause any bond-breaking reactions in the model. Lastly, O_3 and RNS are not included as the applied force field is not able to describe the interactions of these species correctly. [38]

The advantage of MD simulations is that no assumptions need to be made regarding the interaction mechanisms that take place, so they are ideally suited to study complex chemical reactions. Indeed, the interaction processes follow automatically from the force field and the integration of the equations of motion.

The potential energy of the system is determined by the spatial distribution of all atoms in the system. Because we describe the individual atoms in the system, we can only simulate a small part of the real skin layer in order to avoid excessively long calculation times. We thus construct a simulation box containing a mixture of ceramides, cholesterol molecules and fatty acids, and apply periodic

boundary conditions in the x and y directions, to mimic a larger system. To account for heat dissipation from the box, the Nosé-Hoover thermostat is applied, using a relaxation constant of 25 fs [48, 49], which takes away the extra heat released in exothermic reactions or delivers the energy needed for endothermic reactions. All simulations are carried out at a temperature of 300 K and the MD time-step used in our simulations was set to 0.1 fs.

The simulation box under study, illustrated in figure 1A, is a box of 11 Å x 22 Å x 90 Å, consisting of 9 ceramides, 4 cholesterol molecules and 3 free fatty acids. The arrangement of the different molecules is based on experimental results [41-43]. A schematic representation is shown in figure 1B and the ceramides considered in this model are represented in figure 2. The stratum corneum is represented as a lamellar structure (bilayer) with a periodicity of 45 Å. The upper layer consists of ceramide molecules, while the bottom layer contains ceramides as well as cholesterol molecules. The free fatty acids are placed randomly in between these two layers. CER [EOS], which plays an important role in the formation of this multi-layered structure, is able to span a layer and extend to the adjacent layer. These ceramides are used because they occur most frequently in human SC, as demonstrated experimentally [50]. The free fatty acid in this model system is α-linolenic acid, which is chosen because it serves as a good model for other unsaturated fatty acids that might be present in the SC, since it contains an average number of unsaturated bonds and it has an average carbon chain length.

To construct the simulation box, the different molecules were structured in the *z*-direction as shown in figure 1. In addition, an orthorhombic packing was chosen in the *xy*-plane, as this is the most frequently observed packing in healthy SC [51]. Subsequently, an external pressure was applied in all directions to acquire a density of 1.23 $g.cm^{-3}$, which is in agreement with experimental values [52]. To prevent the entire structure from drifting through space during the simulation, the atoms in the bottom 5 Å were restrained so that they could only move in the *xy*-plane. However, this will not influence the results, as the observed reactions will only occur in the upper 10 Å (see below).

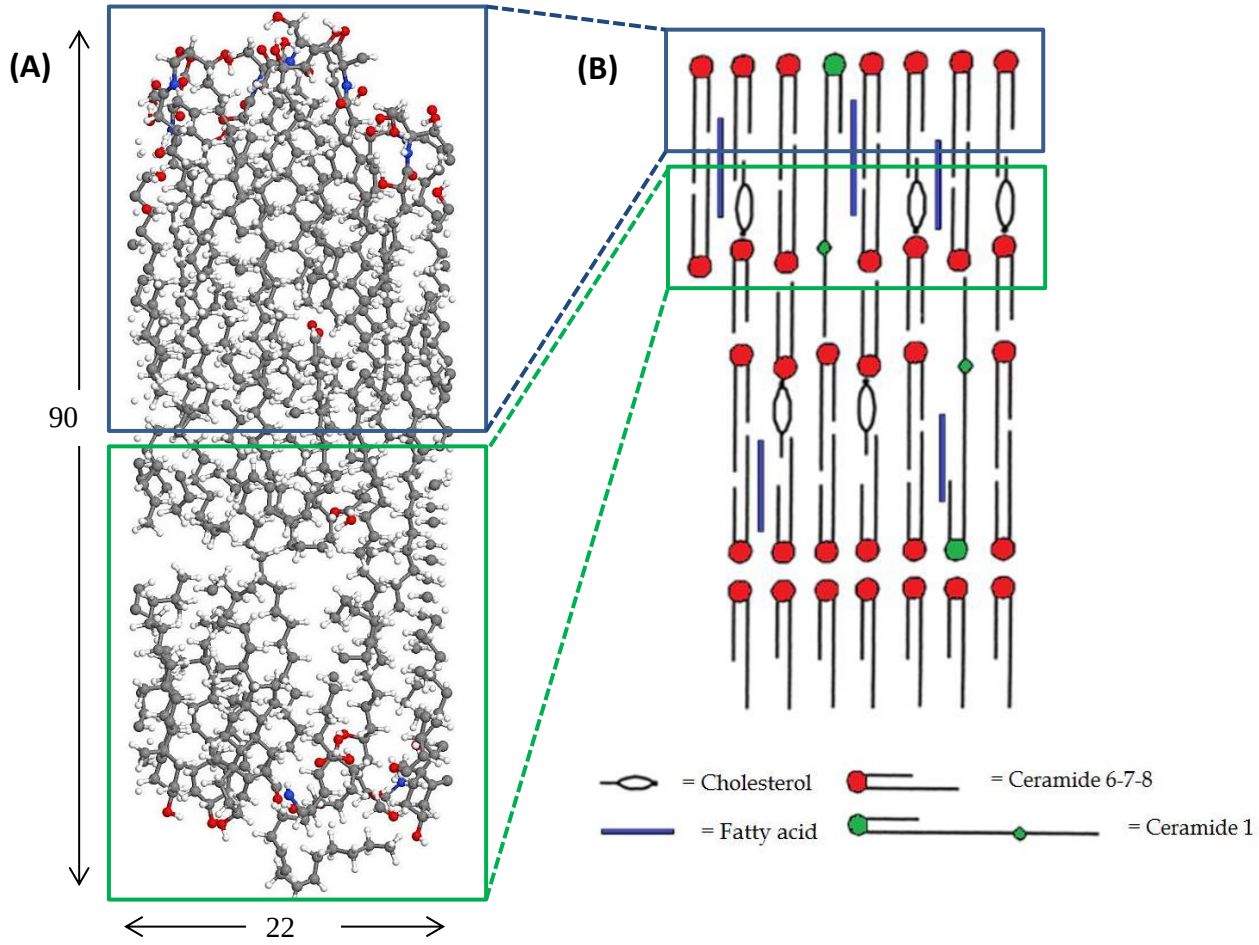

Figure 1: (A) Model system under study. The red, grey, blue and small white spheres represent O, C, N and H atoms, respectively. Periodic boundary conditions are applied in the x and y directions. In figure (B), a schematic representation is shown.

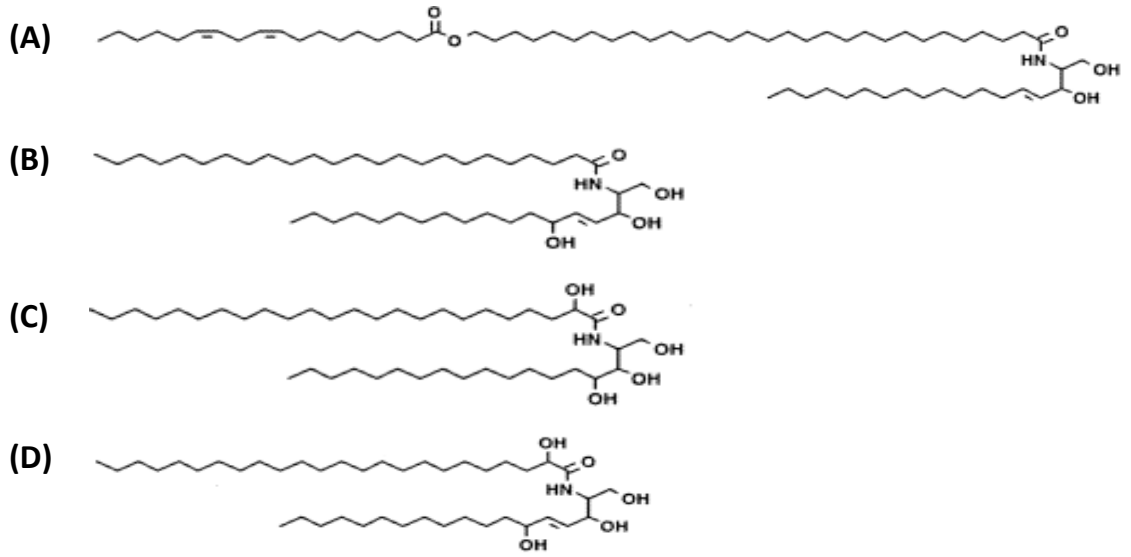

Figure 2: Ceramides included in the model system: CER [EOS] (A), CER [NH] (B), CER [AP] (C) and CER [AH] (D)

The nomenclature of the different ceramides is based on the following rules. The first letter (A, N and EO) refers to the fatty acid chain which is present in the ceramide. A refers to an α-hydroxy fatty acid, N to a non-hydroxy fatty acid, and EO to an esterified ω-hydroxy fatty acid. The last letter (S, H and P) refers to the sphingoid which is present in the ceramide. S refers to sphingosine, H to 6-hydroxy sphingosine and P to phytosphingosine [50].

To investigate the interactions of the model system with OH radicals, which originate from the plasma, 15 OH radicals were placed above the structure (figure 1A) beyond the cutoff of the force field at a distance of 10 Å. All impinging OH radicals were launched towards the target with the same, fixed, initial velocity according to a kinetic energy of 0.026 eV, corresponding to 300 K. The velocity of all other atoms is controlled by the Nosé-Hoover thermostat, ensuring a Maxwellian velocity distribution at a temperature of 300 K. The lateral starting positions of the OH radicals were chosen randomly, while the initial distance from the target was beyond the cut-off of the potential, creating 450 different starting positions over the 30 simulations. The simulation time in each of the simulations was 200 ps.

3. Results

Our calculations predict that as soon as an OH radical interacts with the ceramides, which form the upper layer of the model, a first reaction takes place within 2 picoseconds. Because reactions only occurred in the upper 10 Å of the model system, no reactions were observed with the cholesterol or free fatty acids. The reaction which occurs most is an H-abstraction of an alcohol group, forming H_2O. The total number of H-abstractions observed in our simulations, was 330. In 210 cases (i.e., 64%), no further reaction occurred within the simulation time of 200 ps. In the remaining 36% (i.e., 120 cases), the reaction product reacts further with a new OH radical, and several different reactions may occur, with the formation of either carbonyl functional groups or imines; see Table 1 for the relative occurrence of these reactions. As is clear from this table, the dissociation of a ceramide into two aldehydes occurs most frequently (after a first H-abstraction), meaning that this reaction has the lowest energy barrier of all reactions shown in the table.

In the following sections, these reactions will be discussed, with their corresponding reaction mechanism. To make the schematic representations of the different reactions more clear, only the ceramide which reacts will be shown in each figure.

Table 1: Relative occurrence of the different reactions occurring during the simulations, after a first H-abstraction. The percentage is based on the total number of 120 reactions, proceeding after the first H-abstraction (see text).

Reaction	**Percentage**
Aldehyde formation	28.6 %
Dissociation of ceramide into two aldehydes	42.9 %
Dissociation of ceramide into aldehyde and imine	19.0 %
Formation of formaldehyde	9.5 %

3.1 Aldehyde formation

Figure 3 illustrates aldehyde formation upon two subsequent impacts of OH radicals on a ceramide. The reaction is shown for CER [EOS], but it also occurred with the other ceramides. In the first step, an H atom is abstracted from the alcohol group, which is the most acidic proton present (see green circle in step (B-C)). This creates an O radical on the ceramide, which leaves the system in an unstable configuration. Upon impact of a new OH radical, a second H atom is abstracted from the adjacent C atom (see red circle in step (D)), creating an aldehyde (see blue circle in step (E)). In both H-abstraction reactions, water is formed. Figure 4 illustrates the reaction mechanism of this reaction.

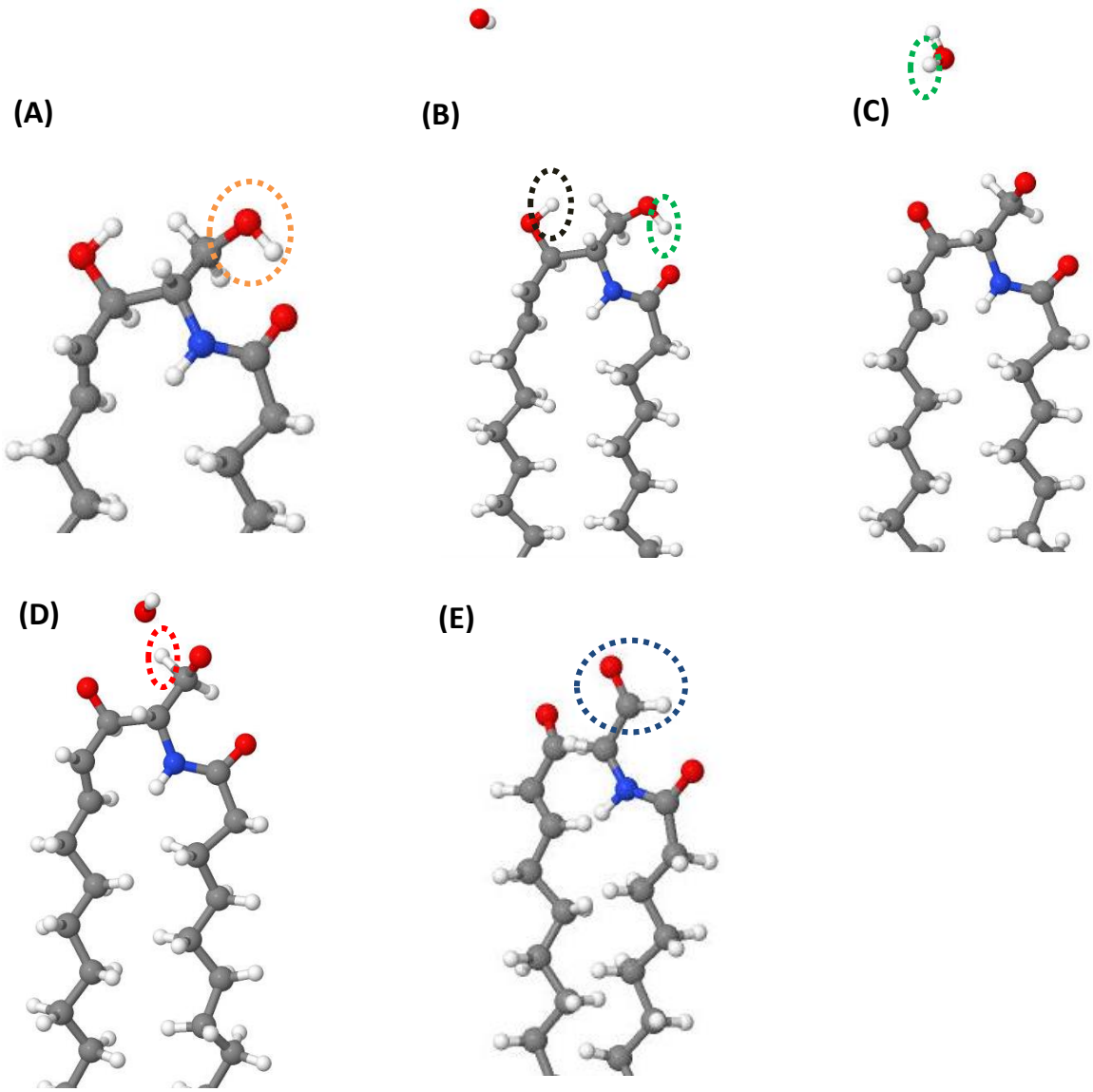

Figure 3: Schematic representation of the oxidation of an alcohol, forming an aldehyde, upon two subsequent impacts of OH radicals on CER [EOS]. In (A) the initial alcohol group is shown (orange circle). In step (B) (at t=6 ps) a first H atom is abstracted, from the OH group of the alcohol (see green circle in step (B-C)). At the same time, an H atom is also abstracted from the second alcohol group in the ceramide (see black circle in step (B)), which is however not important for this reaction, as it simply results in an O radical. In step (D) (at t=45 ps), an H atom from the adjacent C atom is abstracted (see red circle in step (D)), leading to the formation of an aldehyde (see blue circle in step (E)).

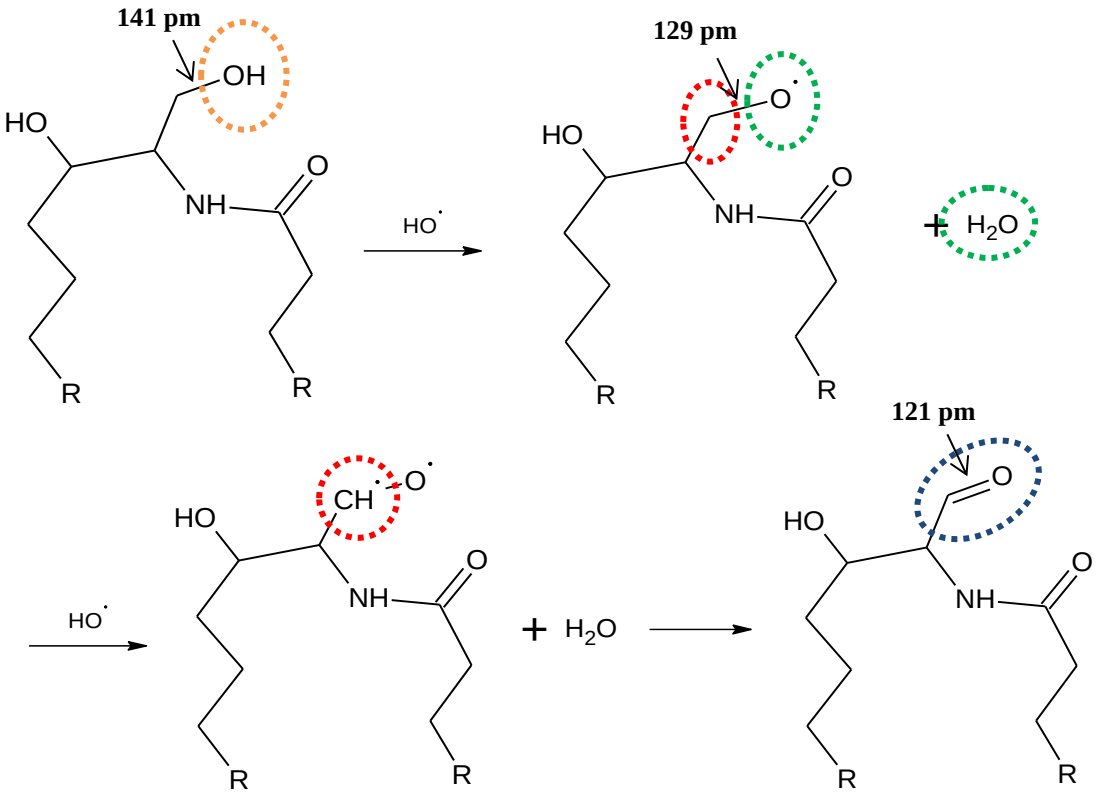

Figure 4: Reaction mechanism of the oxidation of an alcohol to an aldehyde upon two subsequent impacts of OH radicals on ceramide CER [EOS]. The time-averaged bond lengths of the relevant C-O bond are also indicated (see text).

In figure 4, the average bond length of the C-O bond (which is oxidized during the reaction) is indicated, to illustrate that this bond shortens during the reaction (from 1.41 Å to 1.21 Å), which corresponds to the transition from a single to a double bond.

3.2 Dissociation of ceramide CER [AP] into two aldehydes

Figure 5 illustrates the dissociation of ceramide CER [AP], leading to the formation of two aldehydes. Important to note is that this reaction is only possible for CER [AP], due to the need for two vicinal OH groups that are only present in this ceramide. The corresponding reaction mechanism is illustrated in figure 6. In the first step, an O radical abstracts an H atom from the alcohol group (see blue circles in step (A-B)). Note that this O radical can be created in-situ by the reaction of two impinging OH radicals or by H-abstraction from an impinging OH radical due to a ceramide radical. Alternatively, however, the O radical can also be created in other ways in the SC, or directly originate from the plasma.

This H-abstraction from the alcohol group creates a new OH radical plus an O radical on the ceramide. This, or another, OH radical abstracts another H atom from an adjacent alcohol group (see green circles in step (C)). The formed diradical structure dissociates very fast (within 2 ps) which is shown in the last step. Here, the central C-C bond dissociates, forming two aldehydes (see orange circles in step (E)).

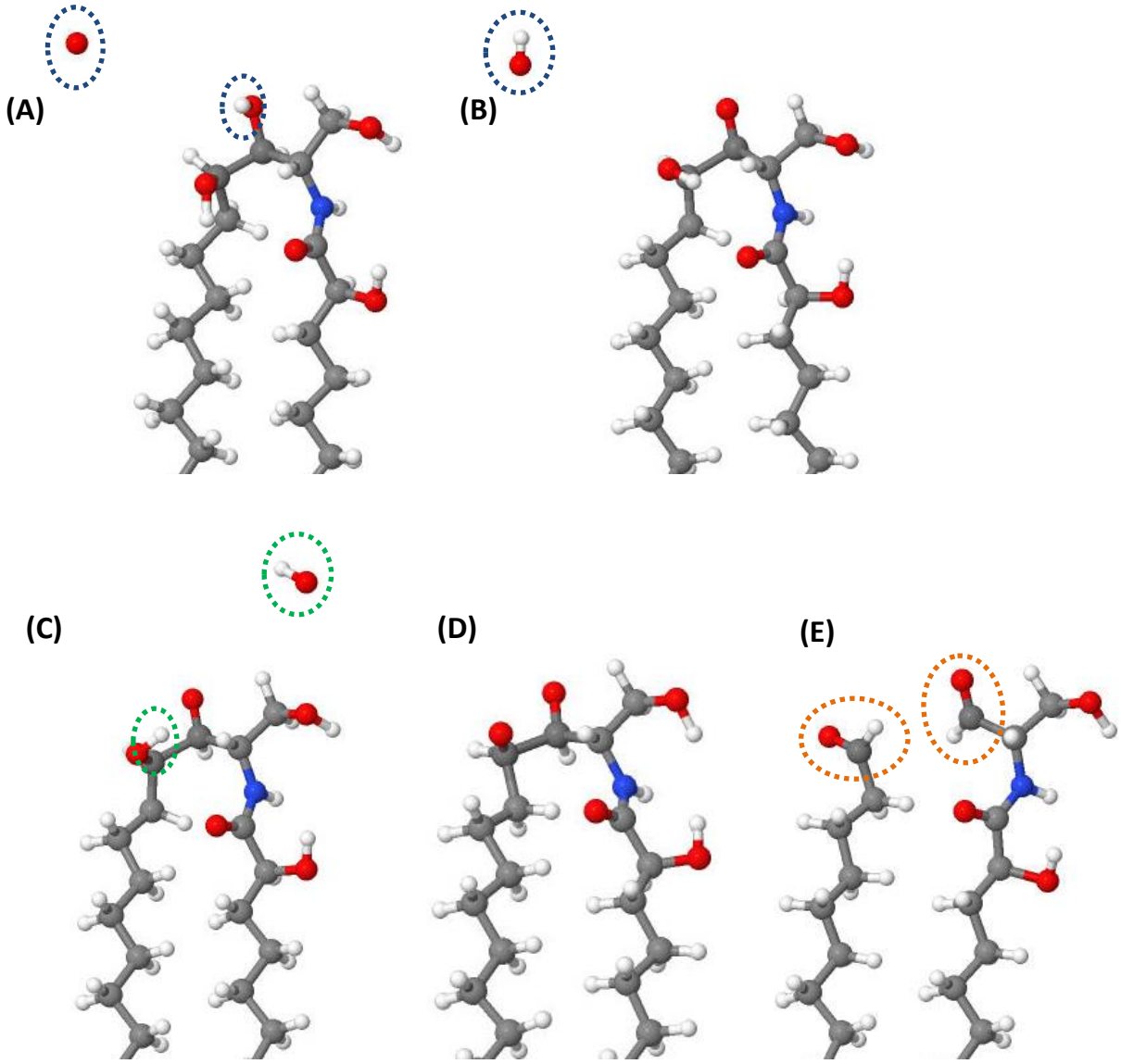

Figure 5: Schematic representation of the dissociation of CER [AP] upon subsequent impacts of an O and an OH radical. In the first step (at t=10 ps), an O radical abstracts an H atom from an alcohol group (see blue circles in step (A-B)). Then (at t=27 ps), another (or the newly formed) OH radical abstracts the H atom from the second alcohol group (see green circles in step (C)). In step (E) (at t=29 ps), the C-C bond is broken, leading to the formation of two aldehydes (see orange circles in step (E)).

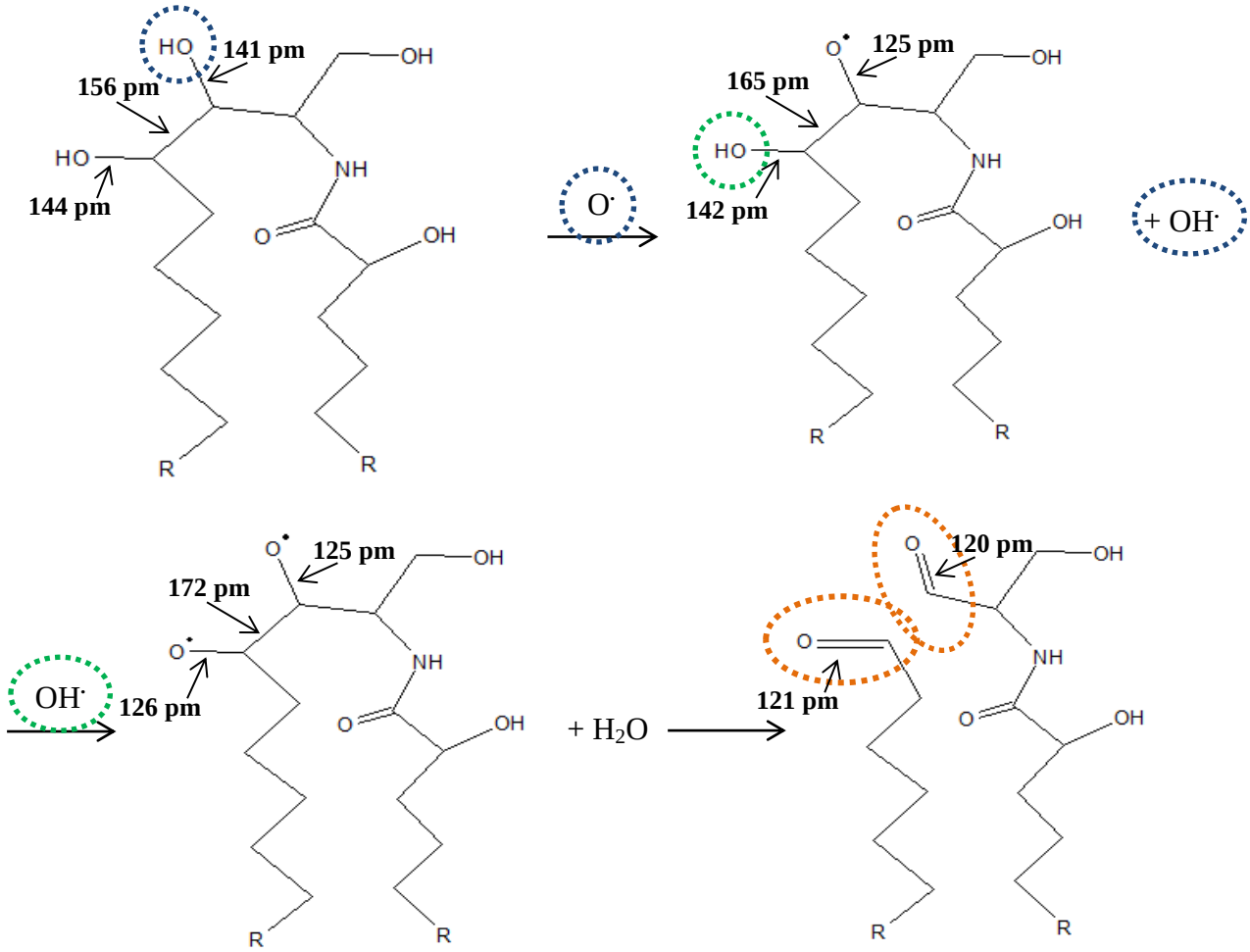

Figure 6: Reaction mechanism of the dissociation of CER [AP] upon impact of an O radical, followed by the impact of an OH radical. The time-averaged bond lengths of the relevant C-O and C-C bonds are also indicated (see text).

In figure 6, the average bond lengths of the bonds involved in the reaction are again indicated. One can see that the bond length of the central C-C bond gradually increases (from 1.56 Å to 1.72 Å) before it eventually breaks. The C-O bond lengths, on the other hand, gradually decrease (from around 1.44 Å to 1.21 Å), indicating the transition from single to double bonds.

3.3 Dissociation of a ceramide into an aldehyde and an imine

Figure 7 illustrates another possible pathway for the dissociation of a ceramide, in this case leading to the formation of an aldehyde and an imine. This dissociation reaction is possible for every ceramide present in the model, because the essential part (a vicinal amino-alcohol group) is present in each of the ceramides. The corresponding reaction mechanism is illustrated in figure 8. In the first step, an OH radical abstracts an H atom from an alcohol group of the ceramide (see green circles in step (A)), again leading to the formation of water and an O radical on the ceramide (see (B)). In the second step, the H of the amine is abstracted by a new OH radical (see orange circles in step (C-D)), resulting in the formation of a new water molecule plus an N radical on the ceramide. This is a very slow step, due to the high stability of the amine. In the final step, which occurs shortly after the previous step, a C-C bond of the ceramide dissociates (see purple circle in step D), leading to the formation of an imine and an aldehyde (see blue circles in step E).

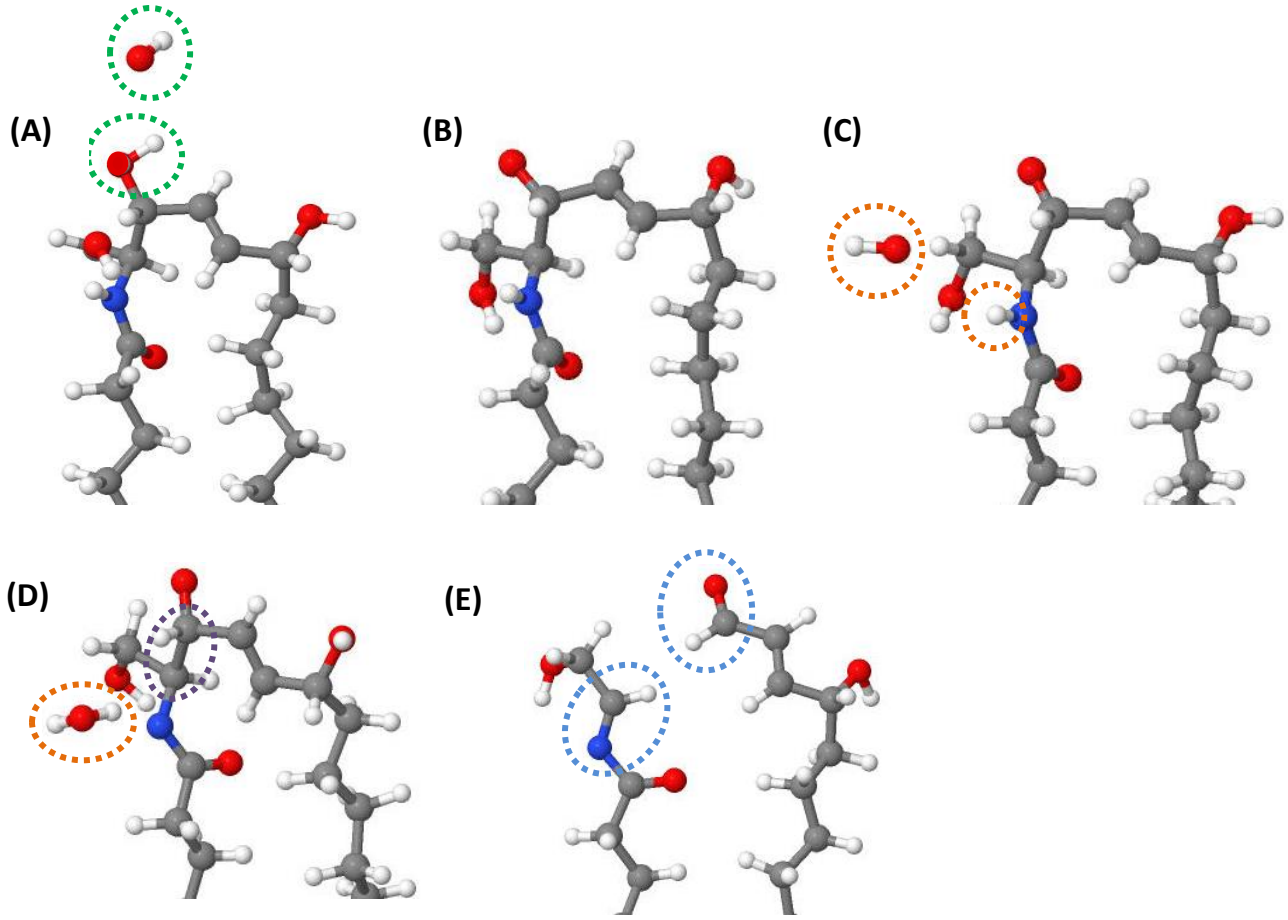

Figure 7: Schematic representation of the dissociation of CER [NH] upon two subsequent impacts of OH radicals. The first step (at t=2 ps) is an abstraction of an H atom from an alcohol group (see green circles in step (A)). Then (at t=108 ps), a new OH radical abstracts the H atom of the amine (see orange circles in step (C-D)). In the final step (at t=120 ps), the ceramide dissociates, leading to the formation of an imine and an aldehyde (see blue circles in step (E)).

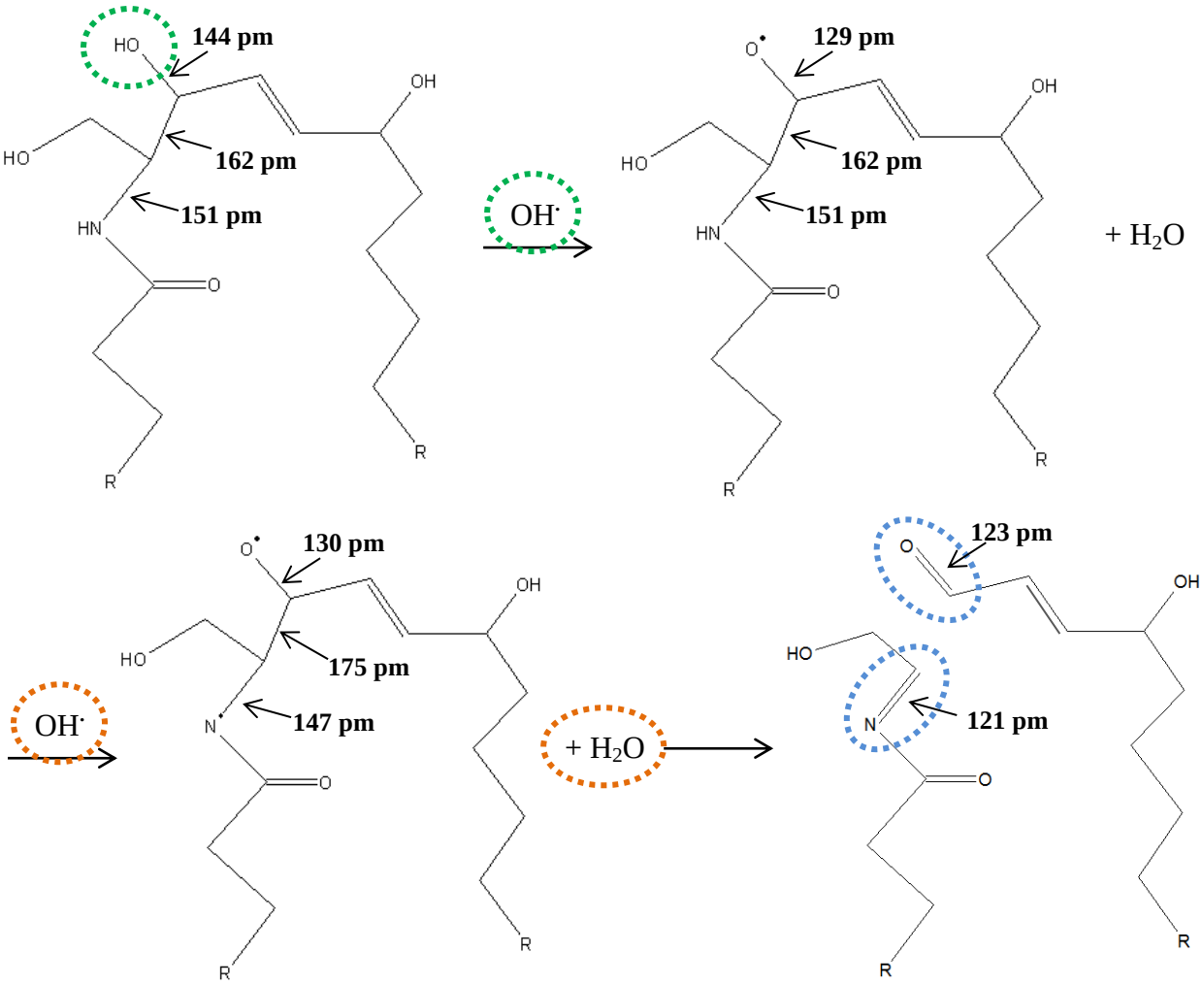

Figure 8: Reaction mechanism of the dissociation of CER [NH] upon two subsequent impacts of OH radicals. The time-averaged bond lengths of the relevant C-C, C-N and C-O bonds are also indicated (see text).

Again, the average bond lengths of the bonds involved in the reaction are shown in figure 8. The central C-C bond becomes longer during the reaction, from 1.62 Å to 1.75 Å, before it eventually breaks. The C-N bond shortens during the reaction, from 1.51 Å to 1.21 Å, corresponding to the transition from an amine (single bond) to an imine (double bond). Similarly, the C-O bond length drops from 1.44 Å to 1.23 Å, also corresponding to the transition from a single to a double bond.

3.4 Formation of formaldehyde

The last reaction which occurred during our simulations, is the formation of formaldehyde upon impact of an O radical, which may again be created upon reaction of two OH radicals (see section 3.2 above) or directly originate from the plasma. This reaction is illustrated in figure 9. The corresponding reaction mechanism is shown in figure 10. In the first step, an O radical abstracts an H atom from an alcohol group of the ceramide (see green circles in step (A-B) in figure 9), leaving an O radical on the ceramide. In the next step, an H atom is abstracted from the amine group by a new OH radical (see blue circles in step (B-C)), which leads to the dissociation of the ceramide and the formation of formaldehyde (see red circles in step (B-C)). The dissociation occurs immediately after the second H-abstraction (i.e. within one picosecond). Due to this dissociation, an imine is formed on the ceramide. This reaction thus proceeds by a mechanism very similar to the one discussed in section 3.3, i.e., a vicinal amino alcohol is oxidized, leading to the cleavage of the central C-C bond.

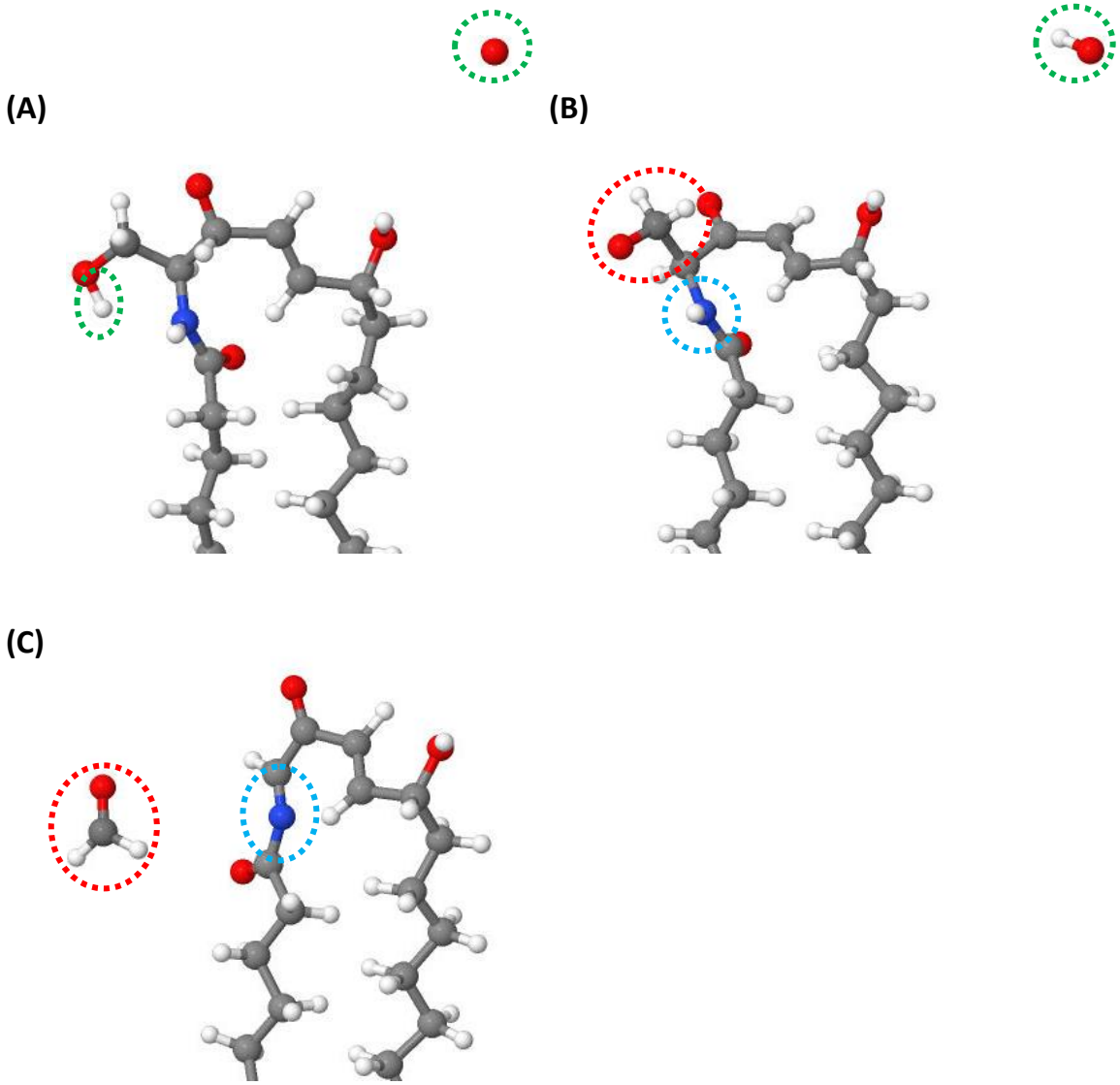

Figure 9: Schematic representation of the formation of formaldehyde upon impact of an O and an OH radical on CER [NH]. The first step (at t=28 ps) is an H abstraction from an alcohol group (see green circles in step (A-B)). Subsequently (at t=38 ps), an H atom is abstracted from the amine group upon impact of the OH radical (see blue circles in step (B-C)), which leads to the dissociation of the ceramide and the formation of formaldehyde (see red circles in step (B-C)).

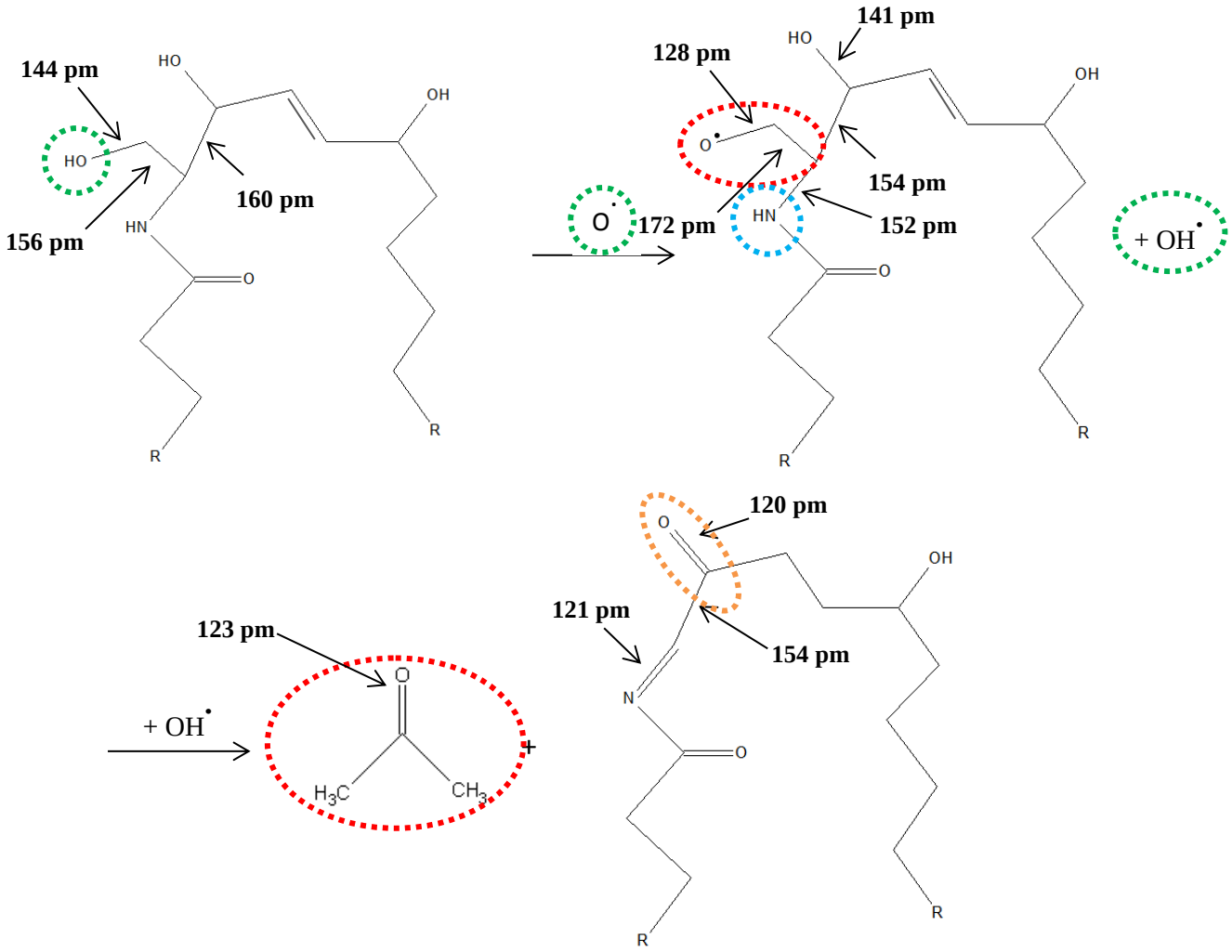

Figure 10: Reaction mechanism of the formation of formaldehyde upon impact of an O and an OH radical on CER [NH]. The time-averaged bond lengths of the relevant C-C, C-N and C-O bonds are also indicated (see text).

In figure 10, the average bond lengths of the bonds involved in the reaction are again indicated for each step. The bond length of the central C-C bond increases from 1.56 Å to 1.72 Å before it eventually breaks. The bond lengths of the C-O and C-N bonds, which are oxidized from single to double bonds (i.e., from alcohol to ketone and from amine to imine, respectively), clearly decrease during the reaction.

4. Discussion

The SC forms the upper layer of mammalian skin tissue and serves as a barrier between the organism and the external environment. This lipid barrier protects the underlying tissue against penetration of harmful substances (i.e., chemicals), infections and water loss. Modifying the structure of the SC may therefore result in a loss of its protective nature and in an increased permeability. It is reported that multiple skin diseases, i.e. atopic dermatitis and ichthyosis [53-56], are (partially) a result of an altered lipid composition in the SC, which often results in the disturbance of the skin function (e.g., dry skin). On the other hand, a temporary and location specific skin permeability proves to be useful in medical applications, like enhancing cutaneous drug delivery [57-59], although in some cases a higher permeability may also increase the risk of infections at the same time.

Our simulations suggest that the reaction of OH radicals with lipids, found in the SC, results in the oxidation of these lipids. Indeed, in all cases we see a drop in the hydroxyl groups and a rise in the carbonyl groups (from C-OH to C=O). The oxidation of the hydroxyl groups goes hand in hand with a drop in C-C bonds in the structure, i.e., we see the formation of aldehyde groups through various reaction pathways, all of which are triggered by H-abstractions. Such oxidation reactions of alcohols into aldehydes are commonly described in the organic chemistry literature (e.g., [60,61]). Also the oxidation of vicinal diols (see section 3.2 above) is a common reaction described in literature [62,63]. Often these reactions are performed using a catalyst to avoid harsh conditions (like the need for free radicals). However, in the case of plasma medicine, free radicals are present, which allow such reactions to proceed more easily.

The observed behaviour, i.e., oxidation of alcohols into aldehydes, is in line with our previous results, where we investigated the oxidation of α-linolenic acid [40], yielding aldehyde formation due to the oxidation of hydroxyl groups, and with experimental results obtained by Marschewski *et al.* [64] and by Klarhöfer *et al.* [65]. Both experimental studies have investigated the interaction between a CAP and the SC or cellulose, respectively. Marschewski *et al.* [64] used X-ray photoelectron spectroscopy to investigate the chemical modification of the lipids found in the SC, before and after plasma treatment. They reported an overall decrease of the aromaticity and the total number of C-C bonds, along with an increased signal corresponding to C-O, C=O, C-N and N-C-O bonds. Indeed, they observed a significant O enrichment of the treated samples, in agreement with the experimental results of Klarhöfer *et al.* [65] for cellulose. Note that we only investigated the interaction with OH radicals (and formed O atoms) while the experimental observations are a result of the synergy between all reactive species originating from the plasma and the treated skin. This might explain why our results do not predict a rise in C-O bonds, which may be the result from reactions between the radicals, found on the unsaturated lipids after H-abstraction, and O_2 originating from the plasma or the atmosphere [66,67].

The oxidation predicted by our simulations also leads to the breaking of important structural bonds in the lipids, i.e., the dissociation of the ceramides (see section 3.2 and 3.3). Note that this may lead to pore formation, increasing the permeability of the treated skin for hydrophilic substances. Indeed, Lademann *et al.* [68] investigated the permeability by applying a dye to the skin, treated with or without CAPs, and the hydrophilic dye showed a higher permeability through the plasma-treated skin, which the authors linked to the changes found in the SC after plasma treatment. Leduc et al. [69] also investigated cell permeabilization upon treatment by a CAP, and reported that the plasma can create pores between 4.8 and 6.5 nm in radius. It should be realized, however, that in our simulations only chemical reactions with the upper 10 Å of the model system are observed. This may be due to the small simulation box, which is necessary to keep the calculation time reasonable (the average calculation time for this model is 1 month). The limited box, together with the short simulation time, prevents the dissociated ceramide parts to drift away from each other. As a result, pore formation is not really observed, making it more difficult for new impinging plasma species to travel deeper into the model structure. Nevertheless, we believe that pore formation, as a result of the dissociation of the ceramides, could in principle arise from our simulations, if the simulation box size and calculation time would be no limiting factors.

Our simulations also predict that formaldehyde may be a possible reaction product of OH interacting with ceramides (see section 3.4). Formaldehyde is widely known as a disinfectant, able to kill many bacteria, viruses and fungi, thus it is able to exhibit an extra sterilizing effect on the treated area, in combination with the ROS of the plasma treatment [36,37,39]. On the other hand, formaldehyde is also a toxic chemical for organisms and can even induce DNA damage in mammalian cells, resulting in cancer [70]. However, due to the high reactivity, formaldehyde is probably consumed in other reactions in the plasma-skin chemistry, and we expect not too many toxic effects to the organism. Nevertheless, more experimental research about the effects of formaldehyde formation by plasma treatment is required.

Finally, multiple studies showed the regeneration of healthy skin, *in vivo*, after plasma treatment, and demonstrated that no macroscopic effects were detected after a low dose of plasma treatment, i.e. no burns, inflammation, itching, or visible macroscopic changes [21,27,68,71]. The combination of the oxidation and enhanced permeability due to the breaking of important structural bonds (as seen in our results), the regeneration of the healthy skin and the sterilizing effect of plasma treatments will prove

to be very interesting for many medical applications for skin treatment (i.e., enhanced drug delivery) with a very low risk of infections or damaging healthy cells.

5. Conclusions

Reactive MD simulations are performed using the Reax force field to study the interaction of OH (and in situ formed O) radicals with an approximate model system for the upper skin layer (i.e., the stratum corneum), consisting of ceramides, free fatty acids and cholesterol.

All observed mechanisms start with H-abstraction from a ceramide. This H-abstraction often starts a cascade of other reactions, eventually leading to the formation of aldehydes, the dissociation of ceramides or the elimination of formaldehyde. These end products will most likely react further with, for example, new impinging radicals. Due to the limited simulation time (200 ps), however, these further reactions were not observed. Note that all ceramides were equally reactive, except for the reaction leading to the dissociation of a ceramide with the formation of two aldehydes; indeed, this reaction requires a vicinal diol, which is only present in CER [AP]. The reactions predicted by our simulations, i.e., the oxidation of alcohols (or vicinal diols) into aldehydes and the dissociation of ceramides, are commonly described in organic chemistry literature.

One possible implication for the skin tissue is the permeabilization of the stratum corneum, due to the dissociation of the ceramides. Indeed, this could result in pore creation in the skin layer. These pores can be beneficial, e.g. when the goal of the plasma treatment is to hydrate dehydrated skin or enhance the delivery of drugs through the skin barrier. This process is for instance observed with cell membranes when a plasma treatment is applied to a cell culture [68,69]. Another important reaction is the elimination of formaldehyde from the skin, which could both be beneficial or harmful for our body. Formaldehyde is known to kill bacteria (i.e., it is used as a disinfectant), but it is also carcinogenic for humans.

The simulations performed in this research helps to achieve a better understanding of the atomic-level processes and mechanisms which occur when plasma species (OH radicals) interact with the upper layer (stratum corneum) of our skin tissue.

Acknowledgements

This work is financially supported by the Fund for Scientific Research Flanders (FWO). The work was carried out in part using the Turing HPC infrastructure of the CalcUA core facility of the Universiteit Antwerpen, a division of the Flemish Supercomputer Center VSC, funded by the Hercules Foundation, the Flemish Government (department EWI) and the Universiteit Antwerpen.

References

[1] Kong M G, Kroesen G, Morfill G, Nosenko T, Shimizu T, van Dijk J and Zimmermann J L 2009 *New J. Phys.* **11** 115012
[2] Ostrikov K, Neyts E C and Meyyappan M 2013 *Adv. Phys.* **62** 113
[3] Fridman G, Friedman G, Gutsol A, Shekhter A B, Vasilets V N and Fridman A 2008 *Plasma Process. Polym.* **5** 503
[4] Morfill G E, Kong M G and Zimmermann J L 2009 *New J. Phys.* **11** 115011
[5] von Woedtke Th, Reuter S, Masur K and Weltmann K D 2013 *Phys. Rep.* **530** 291
[6] Isbary G, Shimizu T, Li Y-F, Stolz W, Thomas H M, Morfill G E and Zimmermann J L 2013 *Expert Rev. Med. Devices* **10** 367
[7] Moisan M, Boudam K, Carignan D, Kéroack D, Levif P, Barbeau J, Seguin J, Kutasi K, Elmoualij B, Thellin O and Zorzi W 2013 *Eur. Phys. J.- Appl. Phys.* **63** 10001
[8] Moreau M, Orange N and Feuilloley M G J 2008 *Biotechnol. Adv.* **26** 610
[9] Laroussi M 2005 *Plasma Process. Polym.* **2** 391
[10] Yousfi M, Merbahi N, Pathak A and Eichwald O 2014 *Fundam. Clin. Pharmacol.* **28** 123
[11] Niemira B A 2012 *Annu. Rev. Food Sci. Technol.* **3** 125
[12] Kim J E, Lee D U and Min S C 2014 *Food Microbiol.* **38** 128

[13] Deng S, Ruan R, Mok C K, Huang G, Lin X and Chen P *J. Food Sci.* **72** M62
[14] Leipold F, Kusano Y, Hansen F and Jacobsen T 2010 *Food control* **21** 1194
[15] Perni S, Shama G and Kong M G 2008 *J. Food Prot.* **71** 1619
[16] Kalghatgi S U, Fridman G, Cooper M, Nagaraj G, Peddinghaus M, Balasubramanian M, Vasilets V N, Gutsol A F, Fridman A and Friedman G 2007 *IEEE Trans. Plasma Sci.* **35** 1559
[17] Kuo S P, Chen C-Y, Lin C-S and Chiang S-H 2010 *IEEE Trans. Plasma Sci.* **38** 1908
[18] Vandamme M, Robert E, Pesnel S, Barbosa E, Dozias S, Sobilo J, Lerondel S, Le Pape A and Pouvesle J-M 2010 *Plasma Process. Polym.* **7** 264
[19] Ninomiya K, Ishijima T, Imamura M, Yamahara T, Enomoto H, Takahashi K, Tanaka Y, Uesugi Y and Shimizu N 2013 *J. Phys. D: Appl. Phys.* **46** 425401
[20] Emmert S, Brehmer F, Hänßle H, Helmke A, Mertens N, Ahmed R, Simon D, Wandke D, Maus-Friedrichs W, Däschlein G D, Schön M P and Viöl W 2013 *Clinical Plasma Medicine* **1** 24
[21] Kramer A, Lademann J, Bender C, Sckell A, Hartmann B, Münch S, Hinz P, Ekkernkamp A, Matthes R, Koban I, Partecke I, Heidecke C D, Masur K, Reuter S, Weltmann K D, Koch S and Assadian O 2013 *Clinical Plasma Medicine* **1** 11
[22] Graves D B 2012 *J. Phys. D: Appl. Phys.* **45** 263001
[23] Zhang Q, Sun P, Feng H, Wang R, Liang Y, Zhu W, Becker K H, Zhang J and Fang J 2012 *J. Appl. Phys.* **111** 123305
[24] Deng X, Shi J and Kong M G 2006 *IEEE Trans. Plasma Sci.* **34** 1310
[25] Kim S J, Chung T H, Bae S H and Leem S H 2009 *Appl. Phys. Lett.* **94** 141502
[26] Lu X, Ye T, Cao Y, Sun Z, Xiong Q, Tang Z, Xiong Z, Hu J, Jiang Z and Pan Y 2008 *J. Appl. Phys.* **104** 053309
[27] Fridman G, Peddinghaus M, Balasubramanian M, Ayan H, Fridman A, Gutsol A, Brooks A and Friedman G 2006 *Plasma Chem. Plasma Process.* **26** 425
[28] Fridman G, Brooks A D, Balasubramanian M, Fridman A, Gutsol A, Vasilets V N, Ayan H and Friedman G 2007 *Plasma Process. Polym.* **4** 370
[29] Kalghatgi S, Dobrynin D, Fridman G, Cooper M, Nagaraj G, Peddinghaus L, Balasubramanian M, Barbee K, Brooks A, Vasilets V, Gutsol A, Fridman A and Friedman G 2008 in Plasma assisted decontamination of biological and chemical agents, ed: Springer, 173-181
[30] Lackmann J-W, Schneider S, Edengeiser E, Jarzina F, Brinckmann S, Steinborn E, Havenith M, Benedikt J and Bandow J E 2013 *J. R. Soc. Interface* **10** 20130591
[31] Bartis E A J, Barrett C, Chung T-Y, Ning N, Chu J-W, Graves D B, Seog J and Oehrlein G S 2014 *J. Phys. D: Appl. Phys.* **47** 045202
[32] Chung T-Y, Ning N, Chu J-W, Graves D B, Bartis E, Seog J and Oehrlein G S 2013 *Plasma Process. Polym.* **10** 167
[33] Bartis E A J, Graves D B, Seog J and Oehrlein G S 2013 *J. Phys. D: Appl. Phys.* **46** 312002
[34] Neyts E C, Yusupov M, Verlackt C C and Bogaerts A 2014 *J. Phys. D: Appl. Phys.* **47** 293001
[35] Bogaerts A, Yusupov M, Van der Paal J, Verlackt C C W and Neyts E C 2014 *Plasma Process. Polym.* DOI: 10.1002/ppap.201400084
[36] Yusupov M, Neyts E C, Khalilov U, Snoeckx R, van Duin A C T and Bogaerts A 2012 *New J. Phys.* **14** 093043
[37] Yusupov M, Bogaerts A, Huygh S, Snoeckx R, van Duin A C T and Neyts E C 2013 *J. Phys. Chem. C* **117** 5993
[38] Yusupov M, Neyts E C, Verlackt C C, Khalilov U, van Duin A C T and Bogaerts A 2014 *Plasma Process. Polym.* DOI: 10.1002/ppap.201400064
[39] Yusupov M, Neyts E C, Simon P, Berdiyorov G, Snoeckx R, van Duin A C T and Bogaerts A 2014 *J. Phys. D: Appl. Phys.* **47** 025205
[40] Van der Paal J, Aernouts S, van Duin A C T, Neyts E C and Bogaerts A 2013 *J. Phys. D: Appl. Phys.* **46** 395201
[41] Kessner D, Kiselev M, Dante S, Hauβ T, Lersch P, Wartewig S, Neubert H H R 2008 *Eur. Biophys. J.* **37** 989
[42] Bouwstra A J, Dubbelaar E R F, Gooris S G, Ponec M 2000 *Acta. Derm. Venereol* **208** 23
[43] Moore J D, Rerek E M 2000 *Acta. Derm. Venereol* **208** 16
[44] van Duin A C T, Dasgupta S, Lorant F and Goddard W A III 2001 *J. Phys. Chem. A* **105** 9396

[45] Buehler M J 2006 *J. Comput. Theor. Nanos.* **3** 603
[46] Chenoweth K, van Duin A C T and Goddard W A III 2008 *J. Phys. Chem. A* **112** 1040
[47] Rahaman O, van Duin A C T, Goddard W A III and Doren D J 2011 *J. Phys. Chem. B* **115** 249
[48] Nosé S 1984 *J. Chem. Phys.* **81** 511
[49] Hoover G W 1985 *Phys. Rev. A.* **31** 1695
[50] Ishikawa J *et al.* 2010 *Journal of Investigative Dermatology* **130** 2511
[51] Pilgram G, Vissers D, van der Meulen H, Pavel S, Lavrijsen S, Bouwstra J, Koerten H 2001 *Journal of Investigative Dermatology* **117** 710
[52] Anderson L R, Cassidy M J 1973 *Journal of Investigative Dermatology* **61** 30
[53] Shimada K, Yoon J-S, Yoshihara T, Iwasaki T, Nishifuji K 2009 *Veterinary Dermatology* **20** 541
[54] Nishifuji K, Yoon J-S 2013 *Veterinary dermatology* (2013) **24** 60
[55] Mu Z, Zhao Y, Liu X, Chang C, Zhang J 2014 *Clinical reviews in allergy & immunology* **47** 193
[56] Yamamoto A, Serizawa S, Ito M, Sato Y 1991 *Archives of Dermatological Research* **283** 219
[57] Rehman K, Zulfakar M H 2014 *Drug Development and Industrial Pharmacy* **40** 433
[58] Kreilgaard M 2002 *Advanced Drug Delivery Reviews* **54** 77
[59] Souto E B, Almeida A J, Muller R H 2007 *Journal of Biomedical Nanotechnology* **3** 317
[60] ten Brink G-J, Arends I W C E and Sheldon R A 2000 *Science* **287** 1636
[61] Enache D I, Edwards J K, Landon P, Solsona-Espriu B, Carley A F, Herzing A A, Watanabe M, Kiely C J, Knight D W, Hutchings G J 2006 *Science* **311** 362
[62] Khenkin A M, Neumann R 2002 *Adv. Synth. Catal.* **344** 1017-1021
[63] Sugimoto H, Spencer L, Sawyer D T 1987 *Proc. Natl. Acad. Sci. USA* **84** 1731-1733
[64] Marschewski M, Hirschberg J, Omairi T, Höfft O, Viöl W, Emmert S, Maus-Friedrichs W 2012 *Experimental Dermatology* **21** 921
[65] Klarhöfer L, Viöl W, Maus-Friedrichs W 2010 *Holzforschung* **64** 331
[66] Niki E, Yoshida Y, Saito Y, Noguchi N 2005 *Biochemical and Biophysical Research Communication* **338** 668
[67] Catalá A 2010 *Biochemical and Biophysical Research Communication* **399** 318
[68] Leduc M, Guay D, Leask R L, Coulombe S 2009 *New J. Phys.* **11** 115021
[69] Lademann O, Richter H, Meinke M C, Patzelf A, Kramer A, Hinz P, Weltmann K D, Hartmann B, Koch S 2011 *Experimental Dermatology* **20** 488
[70] Conaway C C, Whysner J, Verna L K, Williams G M 1996 *Pharmacology & Therapeutics* **71** 29
[71] Isbary G, Morfill G, Schmidt H U, Georgi M, Ramrath K, Heinlin J, Karrer S, Landthaler M, Shimizu T, Steffes B, Bunk W, Monetti R, Zimmermann J L, Pompl R, Stolz W 2010 *The Britisch Journal of Dermatology* **163** 78